Properly Oriented Heparin−Decasaccharide-Induced Dimers Are the Biologically Active Form of Basic Fibroblast Growth Factor[†,‡]

Franklin J. Moy,[§] Michal Safran,[∥] Andrew P. Seddon,[⊥,#] Doug Kitchen,[§] Peter Böhlen,[⊥,○] David Aviezer,[∥] Avner Yayon,*[,∥] and Robert Powers*[,§]

Departments of Structural Biology and Protein Chemistry, Wyeth-Ayerst Research, Pearl River, New York 10965, and Weizmann Institute of Science, Rehovot 76100, Israel

Received October 10, 1996; Revised Manuscript Received January 21, 1997[⊗]

ABSTRACT: Interaction of basic fibroblast growth factor (FGF-2) with heparin or heparan sulfate proteoglycans (HSPGs) is required for receptor activation and initiation of biological responses. To gain insight into the mechanism of activation of the FGF receptor by FGF-2 and heparin, we have used NMR, dynamic light scattering, and HSPG-deficient cells and cell-free systems. The first 28 N-terminal residues in FGF-2 were found to be highly mobile and flexible, consistent with the disorder found in both the NMR and X-ray structures. The structure of an FGF-2−heparin−decasaccharide complex that binds to and activates the FGF receptor was compared to a heparin−tetrasaccharide-induced complex that does not promote an interaction with the receptor. The major change observed upon the addition of the tetrasaccharide to FGF-2 was an increase in the correlation time consistent with the formation of an FGF-2 dimer. The NMR line widths of FGF-2 in the presence of the decasaccharide are severely broadened relative to the tetrasaccharide, consistent with dynamic light scattering results which indicate FGF-2 is a tetramer. The interaction of these heparin species with FGF-2 does not induce a significant conformational change in the overall structure of FGF-2, but small chemical shift changes are observed in both heparin and receptor binding sites. A *trans*-oriented symmetric dimer of FGF-2 is formed in the presence of the tetrasaccharide whereas two *cis*-oriented dimers in a symmetric tetramer are formed in the presence of the decasaccharide. This suggests that the *cis*-oriented FGF-2 dimer is the minimal biologically active structural unit of FGF-2. These data allow us to propose a novel mechanism to explain the functional interaction of FGF-2 with heparin and its transmembrane receptor.

Basic fibroblast growth factor (FGF-2)[1] is a member of a protein family that exhibits a variety of functions related to cell growth and differentiation (Baird & Bohlen, 1990; Basilico & Moscatelli, 1992; Folkman & Klagsbrun, 1987; Miyamoto et al., 1993), and its angiogenic activity has suggested an involvement in wound healing, tumor growth, and cancer (Basilico & Moscatelli, 1992). A common feature of the FGF family is the high affinity toward heparan sulfate proteoglycans (HSPGs) (Miyamoto et al., 1993). The interaction of FGF-2 with HSPG is required for binding to its cell surface tyrosine kinase receptor (FGFR) and is essential for mediating internalization and intracellular targeting through a proposed mechanism of receptor dimerization (Pantoliano et al., 1994; Reiland & Rapraeger, 1993; Roghani & Moscatelli, 1992; Yayon et al., 1991). It has been suggested that HSPG might interact directly with FGFR to facilitate the formation of a trimolecular complex and that the HSPG-induced dimerization of FGF-2 may be important for receptor dimerization (Kan et al., 1993; Ornitz et al., 1992).

Heparin is a heterogeneous mixture of oligosaccharides of varying length and sulfation levels. Until recently, the minimal heparin-derived sequence identified to bind to FGF-2 was a pentasaccharide with 2-*O*-sulfate groups (Maccarana et al., 1993), and a minimum heparin sequence consisting of an octa- or a decasaccharide was required for FGF-2 to bind to its receptor (Ishihara et al., 1993; Ornitz et al., 1992). Ornitz et al. (1995) have suggested that synthetic heparins as small as a disaccharide would bind FGF-2 and promote FGF-2 binding to its receptor. Although the mechanism by which HSPG activates FGF-2 is still unclear, an FGF-2−heparin binding domain consisting of residues K128, R129, K134, and K138[2] has been identified by site-directed mutagenesis (Li et al., 1994; Thompson et al., 1994) and the X-ray structures of the tetra- and hexasaccharide−FGF-2 complexes (Faham et al., 1996). A potential second heparin binding site has been observed in the X-ray structure of FGF-2 complexed with synthetic

[†] This work was supported in part by the Israel Academy of Sciences and Humanities and the Israel Cancer Research Fund.

[‡] We dedicate this paper to the memory of Yasha Gluzman, our colleague, mentor, and friend.

* Corresponding author.

[§] Department of Structural Biology, Wyeth-Ayerst Research.

[⊥] Department of Protein Chemistry, Wyeth-Ayerst Research.

[∥] Weizmann Institute of Science.

[#] Present address: Department of Molecular Sciences, Pfizer, Inc., Groton, CT.

[○] Present address: ImClone System, Inc., New York, NY 10014.

[⊗] Abstract published in *Advance ACS Abstracts,* April 1, 1997.

[1] Abbreviations: FGF-2, basic fibroblast growth factor; FGFR, tyrosine kinase receptor; HSPG, heparan sulfate proteoglycan; SOS, sucrose octasulfate; NMR, nuclear magnetic resonance; 1D, one dimensional; 2D, two dimensional; 3D, three dimensional; HSQC, heteronuclear single-quantum coherence spectroscopy; HMQC, heteronuclear multiple-quantum coherence spectroscopy; TPPI, time-proportional phase incrementation; NOE, nuclear Overhauser effect; NOESY, nuclear Overhauser enhanced spectroscopy.

[2] Numbering for FGF-2 is from amino acid residue 1 deduced from the cDNA sequence encoding the 155-residue form. The mature form is comprised of residues 2−155.

S0006-2960(96)02545-7 CCC: $14.00

heparin-derived di- and trisaccharides (Ornitz et al., 1995). Heparin has also been shown to protect FGF-2 from inactivation from exposure to low pH, elevated temperature, or proteases and to restore bioactivity to inactive growth factor (Gospodarowicz & Cheng, 1986; Pineda-Lucena et al., 1994; Saksela et al., 1988; Sommer & Rifkin, 1989; Westall et al., 1983).

Elucidation of the mechanism of heparin-induced augmentation of FGF-2 binding to its cell surface receptor has been hampered by often contradictory reports most likely related to the complexity and heterogeneous nature of the system. Several mechanisms based on interpretation of experimental evidence have been proposed with a consensus that heparin induces oligomerization of FGF-2 which in turn facilitates receptor dimerization and transmembrane signaling (Mach et al., 1993; Ornitz et al., 1992, 1995; Spivak-Kroizman et al., 1994; Venkataraman et al., 1996). What has eluded our understanding are data that definitively distinguish between an oligomerization event such as adding "beads on a string versus" a defined structural unit required for receptor binding and activation. In previous papers (Moy et al., 1995, 1996) we presented the nearly complete ^{1}H, ^{15}N, ^{13}CO, and ^{13}C assignments, the solution secondary structure, and the high-resolution NMR structure of FGF-2 to comprise the essential foundation for such a study. In this paper, we present the first direct experimental evidence obtained by NMR, independently confirmed by dynamic light scattering and biological relevance established in cell-based and cell-free assays, to propose a specifically oriented heparin−FGF-2 complex.

MATERIALS AND METHODS

Materials. The heparin-derived tetrasaccharide was kindly provided by Robert J. Linhardt, Division of Medicinal and Natural Products Chemistry, University of Iowa (Pervin et al., 1995), and the heparin-derived decasaccharide was kindly provided by Carl Svahn, Department of Organic Chemistry, Pharmacia AB (Aviezer et al., 1994).

NMR Sample Preparation. A 1 mM ^{15}N-FGF-2 sample was prepared as described previously (Moy et al., 1995) and was titrated with a stock solution of heparin-derived tetrasaccharide at a concentration of 3 mg/150 μL in 50 mM potassium phosphate, 2 mM NaN_3, and 90% H_2O/10% D_2O at pH 5.5. 1D ^{1}H and 2D ^{15}N HSQC (Bodenhausen & Ruben, 1980) were collected at a molar ratio of FGF-2 to tetrasaccharide of 1:0.25, 1:0.5, 1:0.75, and 1:1. The titration of each quarter increment was carried out by addition of 9 μL a of tetrasaccharide stock solution to an initial volume of FGF-2 of 600 μL. The concentration of the tetrasaccharide was determined by dry weight, and the concentration of FGF-2 was determined spectrophotometrically [absorbance (0.1% at 280 nm) = 0.964 (Thompson et al., 1994)].

Similarly, a 1 mM ^{15}N-FGF-2 sample was titrated with a decasaccharide at a molar ratio of FGF-2 to the decasaccharide of 1:0.25, 1:0.5, and 1:1. 1D ^{1}H and 2D ^{15}N HSQC were collected at these concentrations.

NMR Data Collection. All spectra were recorded at 25 °C on a Bruker AMX600 spectrometer using a gradient-enhanced triple-resonance $^{1}H/^{13}C/^{15}N$ probe. All heteronuclear NOE, T_1, and T_2 relaxation time measurements were carried out in duplicate for FGF-2. Water suppression in the NOE, T_1, and T_2 experiments was carried out with the WATERGATE sequence and water flip-back pulses (Grzesiek & Bax, 1993; Piotto et al., 1992) . All 2D spectra with ^{15}N indirectly detected dimensions were recorded with the States−TPPI hypercomplex phase increment (Marion et al., 1989) and collected with appropriate refocusing delays to allow for spectra without any phase correction. The heteronuclear ^{15}N NOE, T_1, and T_2 relaxation times for FGF-2 and the FGF-2−tetrasaccharide complex were measured with ^{1}HN and ^{15}N spectral widths of 8064 and 1642 Hz, respectively, with maximum acquisition times of 127 ms (t_2) and 97.4 ms (t_1).

For FGF-2, both the T_1 and T_2 data were collected with 32 transients per increment. The T_1 inversion recovery times were 20, 60, 140, 240, 360, 520, 720, and 1200 ms and the T_2 Carr−Purcell−Meiboom−Gill (CPMG) (Meiboom & Gill, 1958) trains were 8, 24, 40, 56, 72, 104, 152, and 184 ms in duration (Kay et al., 1992; Markley et al., 1971). Recycle delays for T_1 and T_2 experiments were 1.7 and 1.3 s, respectively. Since the NOE measurement requires an equilibrated ^{15}N magnetization for accurate analysis, the recycle time was extended to more than 6 s while 48 transients per increment were collected. In the NOE experiment with presaturation, the proton saturation period was 3 s. ^{1}H saturation was carried out with the use of 180° ^{1}H pulses applied every 5 ms.

For FGF-2 complexed with the tetrasaccharide in a 1:1 ratio, the T_1 inversion recovery times were 20, 80, 180, 300, 420, 600, 860, and 1300 ms, and the T_2 CPMG periods were 8, 24, 40, 56, and 72 ms. All T_1 experiments were collected with 64 transients, and the 20 ms time point was collected twice. Since the T_2 experiment had a lower signal to noise ratio, 96 scans were used and the time point at 40 ms was collected twice.

The ^{15}N-edited NOESY-HMQC experiments were collected as described previously (Moy et al., 1995).

Data Processing and Analysis. Spectra were processed as described previously (Moy et al., 1995) using the NMRPipe software package (Delaglio et al., 1995) and analyzed with PIPP (Garrett et al., 1991) and NMRPipe. Peak heights were automatically assigned for each residue in all 2D spectra after semiautomatically peak picking one 2D spectrum using NMRPipe. T_1 and T_2 values were determined by fitting the measured peak heights to the two-parameter profile $I(t) = I_0 \exp(-t/T_n)$. The Levenberg−Marquardt algorithm (Press et al., 1986) was used to determine the optimum values of T_n by minimizing the goodness of fit parameter $\chi^2 = \sum(I_c(t) - I_e(t))^2/\sigma$, where $I_c(t)$ are the intensities calculated from the fitting parameters, $I_e(t)$ are the experimental intensities, and σ is the standard deviation of the experimental intensities. For the FGF-2 data σ is the standard deviation of the differences between the heights of corresponding peaks in duplicate spectra divided by the square root of 2 (Palmer et al., 1991) whereas for the FGF-2−tetrasaccharide complex σ was set to the root-mean-square baseline noise in the spectra as determined from NMRDraw. The two methods for determining experimental uncertainty were very similar. Uncertainties in T_1 and T_2 measurements were obtained from the covariance matrix generated in the Levenberg−Marquardt algorithm and were used in Monte Carlo simulations for determining the standard deviations for fitting parameters (Farrow et al., 1994; Kamath & Shriver, 1989; Palmer et al., 1991).

The steady-state NOE values for FGF-2 were determined from the ratios of the average intensities of the peaks with and without proton saturation. Since the data for the FGF-2−tetrasaccharide complex were not recorded in duplicate, the steady-state NOE values were determined from the ratios of the intensities of the peaks with and without proton saturation. The standard deviation of the NOE value was determined by the baseline noise (Farrow et al., 1994). The overall correlation time was determined by using residues that had ^{15}N T_1/T_2 ratios within one standard deviation and NOE values greater than 0.6 (Clore et al., 1990a; Clubb et al., 1995; Kay et al., 1989). Three models of the spectral density functions were used to classify five classes of optimized parameters (Clore et al., 1990a,b; Farrow et al., 1994; Kay et al., 1989). Selection of the appropriate spectral density function was determined by initially fitting the data to the simplest spectral density function and only selecting the more complicated spectral density function as required to fit the data (Clore et al., 1990a; Clubb et al., 1995; Powers et al., 1992).

Dynamic Light Scattering. Dynamic light scattering data were collected and analyzed with a DynaPro-801 instrument (Protein Solutions, Inc., Charlottesville, VA). Initially, 150 μL aliquots from free FGF-2, the FGF-2−tetrasaccharide (1:1) complex, and the FGF-2−decasaccharide (1:0.25) complex NMR samples were used for dynamic light scattering analysis. The titration curves were determined by adding aliquots of a 10-fold excess oligosaccharide stock solution to a 0.5 mM FGF-2 sample. The observed molecular weight at each titration step was averaged over 10 data points.

Binding and Cross-Linking of ^{125}I-FGF-2 to Soluble FGFR-1 and to Cells. Conditioned medium from cells secreting FGF receptor-1−AP fusion protein (0.24 OD units/min) was incubated for 45 min at room temperature with rabbit anti-human placental AP antibodies prebound to agarose−protein A beads (Pierce, Rockford, IL). The FGFR-1-coupled beads were washed three times with 1 mL of 20 mM HEPES, pH 7.5, 150 mM NaCl, 1% Triton X-100, and 10% glycerol (HNTG) and incubated with 2 ng/mL ^{125}I-FGF-2 and heparin−oligosacchrides at increasing concentrations for 90 min at room temperature. High-affinity-bound ^{125}I-FGF-2 was determined after three cycles of washing with HNTG and counted in a γ-counter. High-affinity binding of FGF-2 to CHO cells was performed as described by Yayon et al. (1991). Briefly, ^{125}I-FGF-2 and heparin−oligosacchrides at increasing concentrations were incubated with cells for 90 min at 40 °C. Low-affinity-bound FGF-2 was released from the cell surface by a 5 min incubation with a cold solution containing 1.6 M NaCl and 20 mM HEPES, pH 7.4. High-affinity-bound FGF-2 was determined by a 2 M NaCl and 20 mM acetate buffer, pH 4.0, extraction.

Calculation of the FGF-2−Heparin Molecular Model. The FGF-2 tetramer model was generated by starting with the monomer of FGF-2 from a recently solved FGF-2−SOS crystal structure. The dimer of FGF-2 was created by rotating about the Cys78 Sγ−Cβ axis to permit a minimum distance between 128 and 138 heparin binding regions on different FGF-2 units. A heparin model consisting of alternating sulfated glucosamine−glucose structure (obtained from 1hpn.pdb) was positioned on the dimer roughly spanning the hexasaccharide and tetrasaccharide structures of the recent FGF-2−heparin crystal structure (1bfb.pdb and 1bfc.pdb). This dimer model was minimized and subjected to 50 ps of molecular dynamics using the AMBER 4.0 parameter set. The heparin was used as an axis of rotation to form the tetramer of FGF-2. Thus, the tetramer was formed by a rotation around the heparin with some translation to eliminate interatomic distances which were too short and to maintain salt bridges between heparin and the four copies of FGF-2. The tetramer model was subjected to 500 steps of conjugate gradient minimization.

RESULTS AND DISCUSSION

Titration of FGF-2 with a Decasaccharide and Tetrasaccharide. 2D ^{15}N HSQC spectra of FGF-2 and FGF-2 titrated with both the tetrasaccharide and decasaccharide are shown in Figure 1. A severe increase in line widths results upon addition of heparin to FGF-2 (^{15}N T_2 < 36.6 ms). It is important to note that the results are independent of the order of addition. FGF-2 aliquots added to a concentrated (3 mg/150 μL) and 4-fold excess tetrasaccharide sample brought to the same FGF-2 concentration yielded the same broadened NMR spectra.

The major difference between the tetra- and decasaccharide was the comparable extent of their effect on the FGF-2 spectra. While the decasaccharide caused extensive broadening of the 2D ^{15}N HSQC spectra at a 0.25 molar ratio of heparin to FGF-2, it was possible to titrate the tetrasaccharide to a 1:1 molar ratio with FGF-2 and acquire a 2D ^{15}N HSQC spectrum of acceptable quality. A 1D spectrum shows an approximate 50% decrease in signal intensity at a 1:1 molar ratio of the tetrasaccharide−FGF-2 complex relative to the free FGF-2 spectrum. Similarly, a 2D ^{15}N HSQC shows an approximate 80% decrease in signal intensity.

Chemical shifts are sensitive to local changes in protein structure and provide a qualitative analysis of the structural effects of protein−ligand interactions. From the 2D ^{15}N HSQC spectra of FGF-2 and the complex with the tetrasaccharide and decasaccharide (Figure 1) it is apparent that the presence of heparin does not induce any significant structural changes in FGF-2 since most of the observed chemical shifts are nearly identical between the two samples. Some relatively small chemical shift changes or significant perturbations in signal intensity, however, did occur in both FGF-2−oligosaccharide complexes (0.1−0.3 ppm; vector of both ^{15}N and ^{1}HN chemical shift changes). Residues that incurred small chemical shift changes were clustered in two regions of the FGF-2 structure: N36, G37, L127, K128, R129, G131, K134, G136, T139, G140, Q143, K144, and A145, which are in the vicinity of the heparin binding domain as identified by site-directed mutagenesis and the tetra- and hexasaccharide−FGF-2 complex X-ray structures (Faham et al., 1996; Li et al., 1994; Thompson et al., 1994), and E105, L107, S109, N110, N111, and L149, which are in the vicinity of the putative receptor binding domain (Springer et al., 1994; Zhu et al., 1991).

3D ^{15}N-edited HMQC-NOESY spectra were collected for both free FGF-2 and the FGF-2−tetrasaccharide complex. Figure 2 shows strips taken from both the free and complex ^{15}N-edited NOESY spectra, parallel to the F_1 axis, for the amides of residues Thr-130 through Ser-137 which correspond to the FGF-2−heparin binding site. While the data for the FGF-2−tetrasaccharide complex are only marginal, it is still apparent that the NOE data are identical for both spectra. This supports the conclusion that heparin does not

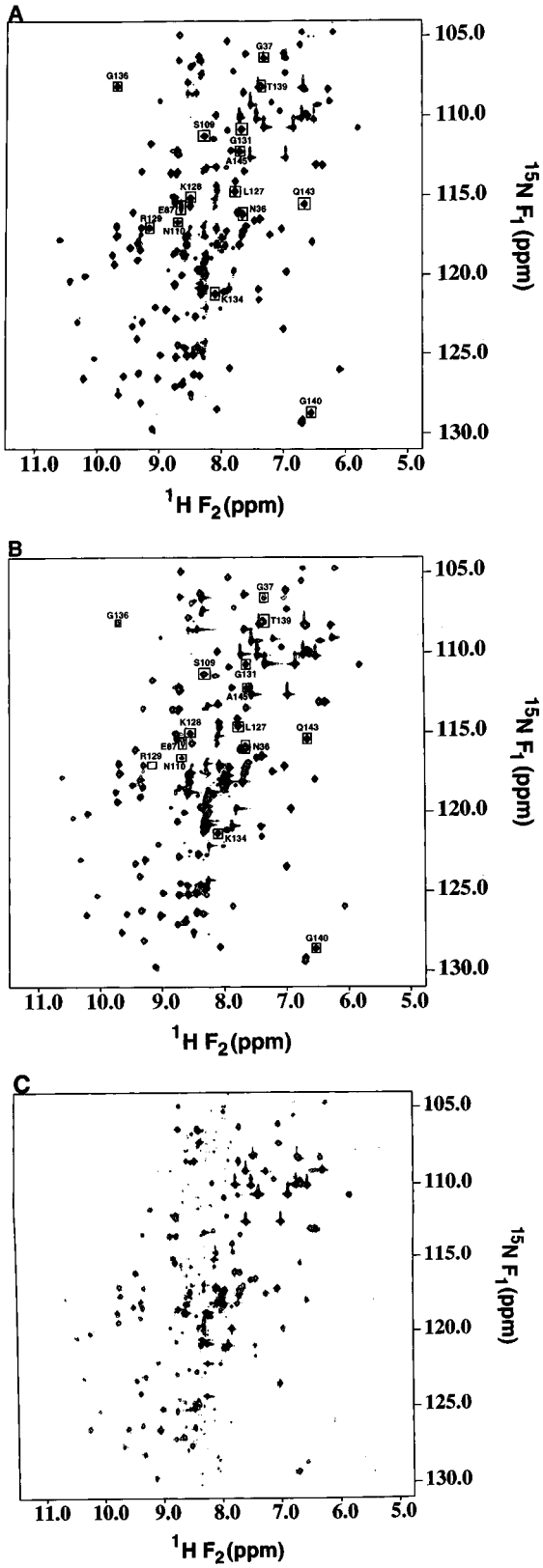

FIGURE 1: Comparison of the ^{1}H−^{15}N HSQC spectra for (A) FGF-2, (B) the 2:1 FGF-2−tetrasaccharide complex, and (C) the 4:1 FGF-2−decasaccharide complex. Residues which incurred a chemical shift change upon addition of the tetrasaccharide are labeled and boxed.

induce any significant conformational change in FGF-2 upon binding and is consistent with the X-ray structures of the tetra- and hexasaccharide−FGF-2 complexes (Faham et al., 1996).

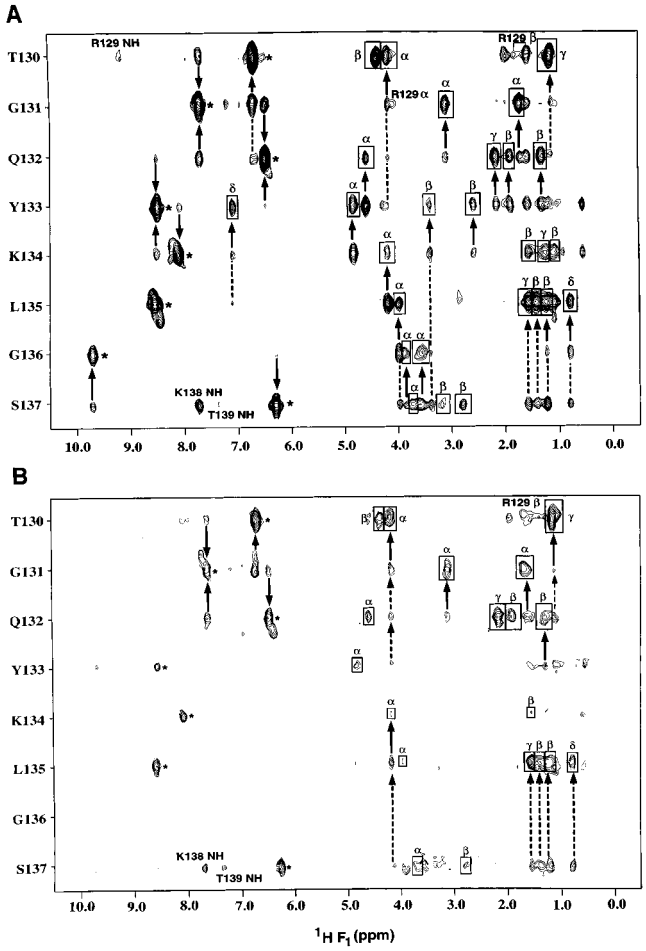

FIGURE 2: Composite of amide strips taken from the 100 ms mixing time 3D ^{15}N-edited NOESY-HMQC spectrum of (A) FGF-2 and(B) the FGF-2−tetrasaccharide complex for the stretch of sequence from Thr-130 to Ser-137 corresponding to missing β-strand XI in the NMR structure (Moy et al., 1995). The diagonal peaks are indicated by an asterisk, NH(i)−NH($i\pm1$), NH($i+1$)−Hα(i), NH(i)−NH($i\pm1$), and NH($i+1$)−Hβ(i) NOEs are indicated by solid arrows, and NH(i)−NH($i\pm2$), NH($i+2,3,4$)−Hα(i), and NH($i+2,3,4$)−Hβ(i) NOEs are indicated by dashed arrows. Intraresidue Hα−NH and Hβ−NH NOEs are boxed.

Although the severe increase in line widths in the FGF-2 NMR spectra upon addition of either the tetra- or decasaccharide implies the formation of high molecular weight forms of FGF-2, it is also possible that the line width increase is a result of a dynamic exchange process. To distinguish between these two possibilities, ^{5}N T_1, T_2, and heteronuclear NOEs were measured for FGF-2 alone and the FGF-2−tetrasaccharide complex to measure the overall correlation time (τ_r) for both samples. Correlation time generally increases linearly with an increase in molecular weight; however, if the effect on line width is a result of dynamic exchange, no effect will be observed on the correlation time and a significant exchange term will be required to fit the relaxation data.

T_1, T_2, and NOE Relaxation Parameters. Relaxation data were obtained for 141 and 125 residues for FGF-2 and the FGF-2−tetrasaccharide complex, respectively, out of 145 possible ^{15}N−^{1}H backbone correlations. Resonance overlap was the main cause of difficulties in measuring peak intensity especially in the random coil region of the T_1, T_2, and NOE spectra. For FGF-2, L92 is overlapped with the intense E14 peak, the peak intensity was assigned to E14, and the

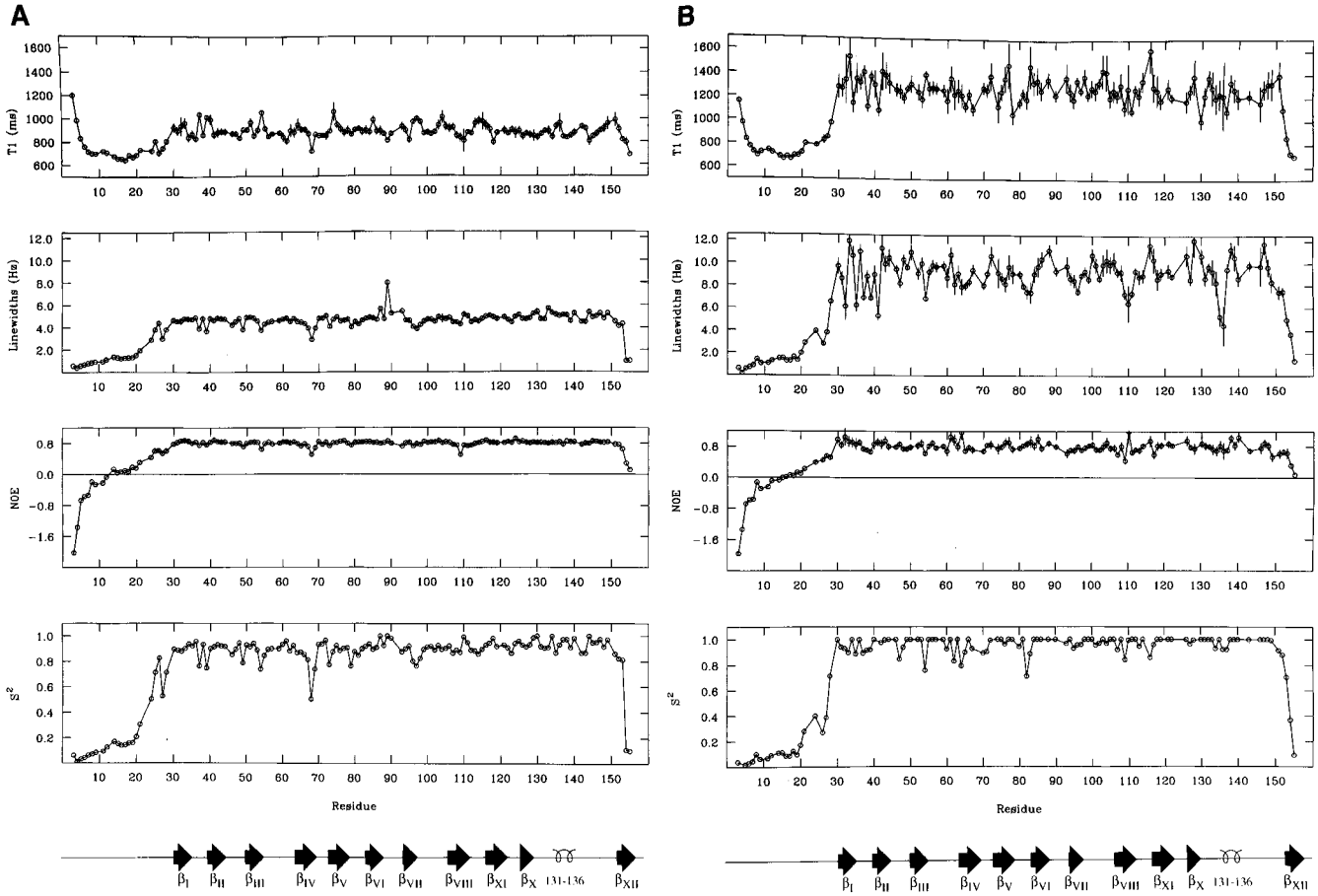

FIGURE 3: Plots of the measured T_1, T_2, and NOE data and the calculated order parameters (S^2) on a per residue basis for (A) FGF-2 and (B) the FGF-2−tetrasaccharide complex. The locations of the 11 β-strands, as determined by NMR (Moy et al., 1995), are indicated below the figures.

relaxation data were not determined for L92. Fewer correlations were obtained in the FGF-2−tetrasaccharide complex because of T_2 line broadening. Relaxation data were not determined for residues E68, R69, S73, A79, G89, L92, Y115, Y120, W123, V125, and G142 in the FGF-2−tetrasaccharide complex because of overlap or weak intensity.

The values of the ^{15}N T_1, T_2, and NOE data are plotted as a function of residue number in Figure 3 for FGF-2 and the FGF-2−tetrasaccharide complex. The average T_1 values for residues 30−152 are 0.894 ± 0.056 and 1.28 ± 0.10 s for FGF-2 and the FGF-2−tetrasaccharide complex, respectively. Similarly, the average T_2 values are 68.5 ± 7.3 and 36.1 ± 7.1 ms and the average NOE values are 0.800 ± 0.057 and 0.809 ± 0.123 for FGF-2 and the FGF-2−tetrasaccharide complex, respectively. A comparison of the experimental ^{15}N T_1 and T_2 data of selected residues for both FGF-2 and the FGF-2−tetrasaccharide complex is shown in Figure 4. Six residues (Y33, C34, L41, F103, R116, and Y124) in FGF-2 had NOE values which exceeded the theoretical maximum of 0.83 by less than 0.04 (Kay et al., 1989). Nine residues (K30, I43, K61, L64, M85, N110, A126, K138, and G140) in the FGF-2−tetrasaccharide complex had NOE values which exceeded the theoretical maximum by less than 0.15. Negative NOEs were observed for residues 3−12 and 3−15 for FGF-2 and the FGF-2−tetrasaccharide complex, respectively.

Calculated Correlation Time (τ_r) for FGF-2 and the FGF-2−Tetrasaccharide Complex. The overall correlation time (τ_r) can be determined from the T_1/T_2 ratio under conditions where the internal correlation time (τ_e) is less than 100 ps, $\tau_r > 1$ ns, and T_2 is not significantly shortened by chemical

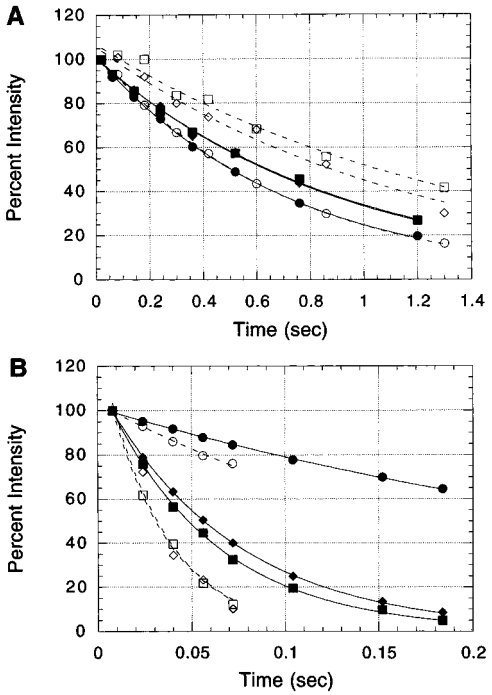

FIGURE 4: Comparison of the experimental ^{15}N (A) T_1 and (B) T_2 data of selected residues of FGF-2 (solid line) and the FGF-2−tetrasaccharide complex (dashed line) with the single-exponential least-squares best-fit curves.

exchange (Clore et al., 1990a; Kay et al., 1989). Thus residues which are suspected to have significant contributions to their experimental T_1 and T_2 values from τ_e and/or chemical exchange are removed from the τ_r calculation. Typically, residues with NOE values less than 0.6 or T_1/T_2 ratios which lie either 1 SD above or below the mean were removed from the τ_r calculation. For FGF-2, 23 residues had NOE values less than 0.6, and 27 residues were outside 1 SD of the T_1/T_2 mean. The overall correlation time for FGF-2 was determined to be 11.4 ± 0.3 ns by fitting the T_1, T_2, and NOE data for each of the 91 residues to the Lipari and Szabo "model-free" formalism (Lipari & Szabo, 1982). The optimal correlation time (τ_r), order parameter (S^2), and effective internal correlation time (τ_e) were calculated individually for each residue, and the overall correlation time for FGF-2 was the average from all the residues. For the FGF-2−tetrasaccharide complex, 27 residues had NOE values less than 0.6, 20 residues were outside 1 SD of the T_1/T_2 mean, and an additional 19 residues did not converge during the τ_r calculation. The optimal overall correlation time for the FGF-2−tetrasaccharide complex was determined to be 20.2 ns by simultaneously fitting the T_1, T_2, and NOE data for 49 residues to the Lipari and Szabo model-free formalism (Lipari & Szabo, 1982). For the FGF-2−tetrasaccharide complex an optimal overall correlation time instead of an average value is reported because of an apparent limitation in the model. A plot of χ^2 versus correlation times (Supplementary Information, Figure 1S) is very asymmetric and flat about the minima. This suggests that certain parameters have a minimal contribution to reducing the value of χ^2 at higher values of τ_r. This results in the mean correlation time of 21.3 ± 1.9 ns being skewed toward a higher value relative to the optimal correlation time of 20.2 ns (minima on the χ^2 versus correlation time plot). This was not the case for free FGF-2 where the mean correlation time of 11.4 ± 0.3 ns was nearly identical to the optimal correlation time of 11.3 ns and the χ^2 versus correlation time plot was symmetrical about the minima. Correlation times of 11.4 and 20.2 ns were used in all subsequent calculations for FGF-2 and the FGF-2−tetrasaccharide complex, respectively.

FGF-2 Dynamics. The generalized order parameter S^2 is plotted as a function of residue number for FGF-2. The average value of the order parameter S^2 for residues 30−152 for free FGF-2 is 0.90 ± 0.05. Other proteins of similar size, including interleukin-4 (Redfield et al., 1992) and p53 (Clubb et al., 1995), have $S^2 \approx 0.90$, indicating limited conformational flexibility. The ^{15}N relaxation data of FGF-2 indicate that the first 28 N-terminal residues are highly flexible and mobile ($S^2 < 0.6$). Negative NOEs were observed for residues 3−12 and 2−25, and 27 residues were best fitted to the extended spectral density model (Clore et al., 1990a,b) in which there are two internal motions. The dynamic analysis supports the previous observation that two distinct conformations exist for the first 28 residues caused by a *cis*−*trans* isomerization of prolines 10 and 13 (Moy et al., 1995) and that the first 17−28 residues are disordered in the NMR structure of FGF-2 (Moy et al., 1996). This is also consistent with the observation that the first 17−19 residues in the X-ray structures of FGF-2 (10−155) are not visible in the electron density map and have been identified as disordered (Ago et al., 1991; Eriksson et al., 1991, 1993; Zhang et al., 1991; Zhu et al., 1991). Aside from the N- and C-terminal regions, FGF-2 is well ordered with all S_2 values being greater than 0.80 except for residues G37, F39, E54, E68, and G70, which are in or near loop regions. Residues G37 and E54 reside in loop regions between β-strands 1 and 2 and β-strands 3 and 4, respectively. Residues E68 and G70 are in the loop between β-strands 4 and 5, and F39 is at the start of β-strand 2. Five other residues in loop regions which were not assigned because of overlap or lack of an observable cross peak were L91, L92, and Y120. All residues exhibit very fast internal motions on time scales ≤20 ps except for residues E54, E67, E68, S96, E108, S109, N111, and Y112, which exhibit internal motions of 20 −111 ps, and the mobile N- and C-terminal residues 1−29 and 152−154, which exhibit a second slower motion on a time scale of 0.3−1.4 ns. The average calculated t_e relative error estimate was 28%.

FGF-2−Heparin Dynamics. The ^{15}N relaxation data (Figures 3 and 4) from the FGF-2−tetrasaccharide complex indicated that the presence of heparin bound to FGF-2 induced a distinct effect on the dynamics of FGF-2. It is quite apparent that the observed T_1 and line width values increased dramatically for residues 30−152 in the FGF-2−tetrasaccharide complex while the NOE values and order parameters were quite similar. The FGF-2−tetrasaccharide complex exhibits the same mobility as free FGF-2 for the N- and C-terminal residues as indicated by order parameters below 0.8. The average value of the order parameter S^2 observed for residues 30−152 for FGF-2 increased in the presence of the tetrasaccharide to 0.96 ± 0.06. An increase in S^2 is not unexpected upon formation of a complex, but there is no indication of a local effect on mobility since the order parameter increase is observed throughout the protein. Therefore, the major effect of the tetrasaccharide on FGF-2 dynamics is the substantial increase in the protein's overall correlation time. Since a correlation time of 20.2 ns was measured for the complex compared to 11.4 ns for free FGF-2, this indicates that the presence of the tetrasaccharide induces the formation of FGF-2 dimers and the observed increase in FGF-2 line widths is not a result of exchange broadening. In the FGF-2−tetrasaccharide complex a total of 18 residues exhibit internal motions of 20−111 ps compared to 8 residues in free FGF, and 9 residues in addition to the mobile N- and C-terminal residues exhibit a second slower motion on a time scale of 0.3−1.4 ns. In addition, an exchange term was required to fit 32 residues for the complex, but only 5 residues in free FGF-2 required this additional exchange term. The average exchange value in the FGF-2−tetrasaccharide complex was 5.4 ± 2.7 Hz. Since an additional exchange term was required by residues throughout the protein structure, this suggests a possible slow monomer−dimer exchange where the dimer is the predominant species.

In the case of the FGF-2−decasaccharide complex, a greater effect was observed on the broadening of FGF-2 line widths compared to the tetrasaccharide. Since the dynamics data for the tetrasaccharide support the formation of a dimer, it is reasonable to conclude that the greater increase in line widths associated with the decasaccharide at a lower molar ratio of decasaccharide to FGF-2 (0.25:1) is consistent with the formation of a higher order oligomer.

FGF-2−Heparin Dynamic Light Scattering. To independently confirm the NMR results, dynamic light scattering data were collected on 150 μL aliquots of the NMR samples

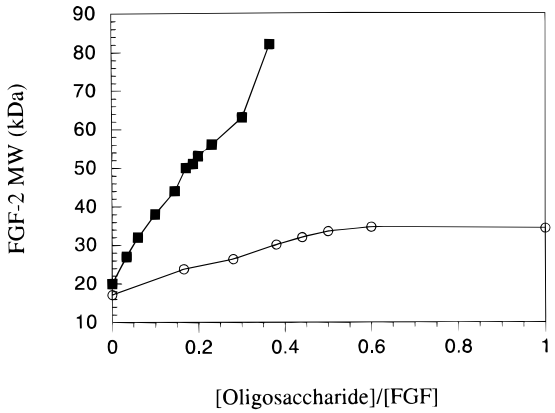

FIGURE 5: Dynamic light scattering results of FGF-2 titrated with the (○) tetrasaccharide and (■) decasaccharide. At higher decasaccharide concentrations significant precipitation occurs.

of FGF-2 and the FGF-2−oligosaccharide complexes. The molecular weights determined indicated that FGF-2 is monomeric, the FGF-2−tetrasaccharide complex is dimeric, and the FGF-2−decasaccharide is tetrameric, which is in accord with the additional overall increase in complexation observed by NMR (Figure 5). This supports the previous conclusion that the observed increase in the FGF-2 NMR line widths caused by the addition of the oligosaccharides is a result of the formation of high molecular weight forms of FGF-2 and not a result of exchange broadening. This is also consistent with the observation that the FGF-2 binding affinity for heparin is relatively strong (K_D in the nanomolar range) and an exchange between free and complexed FGF-2 is not expected on the NMR time scale (Moscatelli, 1987; Nugent & Edelman, 1992; Li & Seddon, 1994; Spivak-Kroizman et al., 1994).

No evidence to suggest an FGF−FGF dimer interface for the tetrasaccharide-containing complex was observed, and the interaction between FGF-2 and the oligosaccharides was determined to occur predominantly in the heparin binding domain. Since the NMR spectra of FGF-2 in the presence and absence of the oligosaccharides are almost identical, this requires the structures of the FGF-2 dimer and tetramer to be composed of symmetric protein units arranged in a conformation such that the backbone atoms are in almost identical environments. Given these constraints, a "sandwich" motif of the FGF-2−tetrasaccharide dimer is indicated which is repeated in the decasaccharide complex. Consistent with a sandwich model, dynamic light scattering data of FGF-2 titrated with both the tetra- and decasaccharide (Figure 5) indicate that complete dimerization of FGF-2 occurs at approximately a 1:0.5 ratio of FGF-2 to the tetrasaccharide and the FGF-2 tetramer occurs at approximately a 1:0.25 ratio.

In Vivo and in Vitro Heparin-Induced FGF-2 Receptor Binding. The ability of both the tetrasaccharide and the decasaccharide to induce high-affinity FGF-2 receptor binding was examined by utilizing two experimental systems: Chinese hamster ovary (CHO) mutant cells deficient in HSPGs and genetically engineered to express FGF receptor-1 (FGFR-1) (Aviezer et al., 1994) and a cell-free *in vitro* system employing the soluble ectodomain of FGFR-1 genetically fused to alkaline phosphatase (Ornitz et al., 1992; Yayon et al., 1992). As shown in Figure 6, both experimental systems demonstrate that the heparin-derived tetrasaccharide was unable to augment ^{125}I-FGF-2 binding to

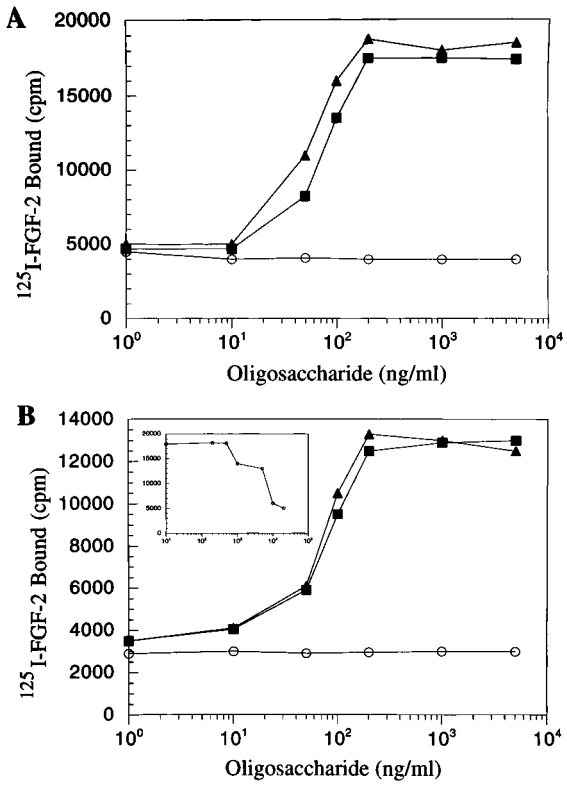

FIGURE 6: ^{125}I-FGF-2 binding to the high-affinity receptor in (A) a cell-free *in vitro* system and (B) CHO mutant cells deficient in HSPG and expressing FGFR-1 in the presence of (▲) heparin, (n) heparin-derived decasaccharide, and (○) heparin-derived tetrasaccharide. (B) The inset shows the effect of the tetrasaccharide in the presence of subsaturating concentrations (100 ng/mL) of decasaccharide-induced FGF-2 binding to the soluble receptor.

the high-affinity receptor while the decasaccharide restored 80−90% of FGF-2 high-affinity receptor binding induced by native heparin. The tetrasaccharide was inactive in both systems even at extremely high concentrations of the tetrasaccharide. Moreover, the "nonactive" tetrasaccharide markedly inhibited in a dose-dependent manner the induced binding of FGF-2 to soluble FGFR-1 at subsaturating concentrations (100 ng/mL) of the decasaccharide (inset, Figure 6B). These results clearly indicate that both oligosaccharides can efficiently bind FGF-2 but only the decasaccharide can further induce high-affinity receptor binding and activation.

Model of a Biologically Active FGF-2−Heparin Complex. The use of NMR in conjunction with dynamic light scattering and receptor binding assays allows us to propose a novel mechanism for the interaction of FGF-2 with heparin and its receptor as illustrated in Figure 7. Since the FGF-2−tetrasaccharide *trans*-dimer is inactive in receptor binding and initiation of the biological response, we conclude that the minimum active structural unit of the FGF-2−heparin complex is the properly oriented *cis*-dimer component of the tetramer sandwich motif induced by the decasaccharide (Figure 7). It is still plausible that the tetramer structure is required for biological activity; in fact, a recent paper by Mohammadi et al. (1996) suggests that autophosphorylation of FGFR requires an association of receptor dimers induced by a multivalent heparin−FGF complex, which is consistent with the tetramer structure induced by the decasaccharide. The observed sandwich motif may be attributed to the presence of both 2-*O*-sulfate and 6-*O*-sulfate groups in the

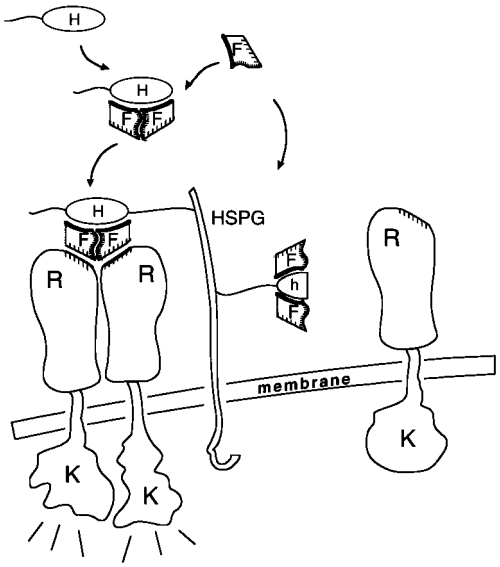

FIGURE 7: Proposed model for the interaction of FGF-2 with the tetrasaccharide to form the inactive *trans*-dimer and with the decasaccharide to form the active *cis*-dimer complexed with the FGF-2−tyrosine kinase receptor dimer.

oligosaccharide, resulting in two distinct charged surfaces for FGF-2 binding. Since the high-affinity binding of heparin to FGF-2 and resulting biological activity are dependent mainly on the presence of 2-*O*-sulfate groups (Maccarana et al., 1993), the observed tetramer structure may simply be a result of the presence of 6-*O* sulfate groups and, therefore, not crucial for activity.

The direct experimental evidence presented here is in full agreement with the previously observed heparin length and charge dependency for FGF-2 receptor mediated activity. Heparin species smaller than an octasaccharide are unable to form the FGF-2 *cis*-dimer or tetramer complex (Aviezer et al., 1994; Ishihara et al., 1993; Ornitz et al., 1992). On the basis of this scheme an FGF-2−decasaccharide tetramer model was generated from an FGF-2−sucrose octasulfate crystal structure, a heparin NMR structure, and the tetra- and hexasaccharide−FGF-2 complex X-ray structures using molecular modeling and molecular dynamics techniques (Figure 8) (Xu et al., 1996). This model is consistent with the chemical shift perturbations observed for the binding of the decasaccharide to the FGF-2-heparin binding site while maintaining a symmetric tetramer structure without modifications to the backbone structure of FGF-2. The model also supports the observation that a decasaccharide would be the shortest oligosaccharide capable of facilitating an active, high-affinity complex of two correctly oriented dimers in a tetramer arrangement by spanning adjacent monomer heparin binding sites. Additionally, residues previously identified as important in receptor binding (Springer et al., 1994; Zhu et al., 1991) are located on exposed surfaces in the FGF-2−decasaccharide tetramer model. These residues are apparently not involved in the FGF−FGF dimer interface or heparin binding site but are adjacent to the FGF-2−heparin binding domain and incur a chemical shift perturbation upon binding heparin. Mutation of E105 (Zhu et al., 1991) and N110 and L149 (Springer et al., 1994) to alanine has been shown to dramatically impact receptor binding affinity. Interestingly, oligosaccharide binding to FGF-2 induces chemical shift perturbations in a region of the protein that forms a receptor binding face but is not directly involved in heparin−FGF-2 interactions. It is tempting to speculate that these local changes in FGF-2 structure contribute to the heparin−dependent ligand−receptor recognition process.

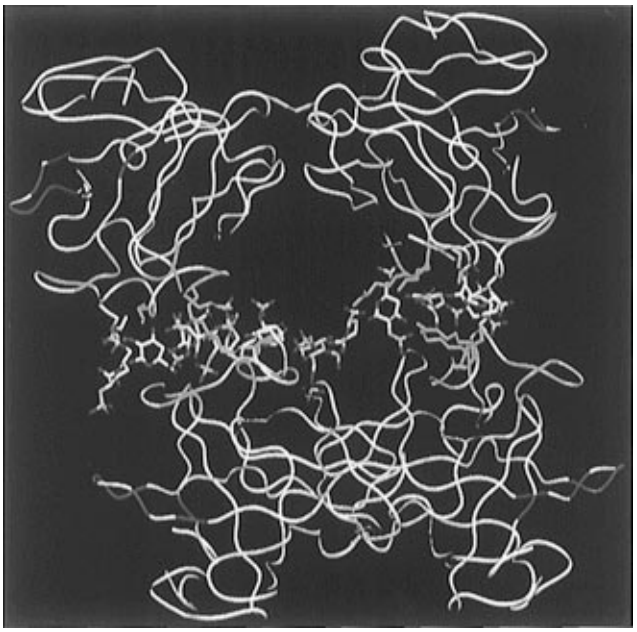

FIGURE 8: FGF-2−decasaccharide tetramer model. The residues involved in heparin binding (128, 129, 134, and 138) are indicated by the presence of side-chain atoms, the potential intermolecular disulfide bond by C78 is colored yellow, the residues that incur chemical shift changes in the heparin binding site are colored blue, and those in the putative receptor binding site are colored red.

Formation of disulfide-linked monomers in the presence of heparin may be a mechanism to enhance the stability of the active heparin−FGF-2 complex. It is interesting to note that C78 in the FGF-2−decasaccharide tetramer model is capable of forming an intermolecular disulfide bond between adjacent monomers, but direct evidence for this disulfide bond was not available since a C78S,C96S-FGF-2 mutant was used for the current study. C78 is also surface accessible, which is consistent with the observation that modification of C78 does not impair receptor binding or activation (Lappi et al., 1991). This suggests that *if* a C78 intermolecular disulfide bond is formed in the presence of heparin, this bond is not crucial or necessary for FGF-2 activity.

FGF-2 dimers have been observed in cross-linking experiments but at very high heparin to FGF-2 concentrations where the major species present was a monomer (Ornitz et al., 1992, 1995). Dimers have been inferred from crystallographic data based on unit cell contacts (Venkataraman et al., 1996) even though X-ray structures of FGF-2 indicate that the protein is a monomer (Ago et al., 1991; Eriksson et al., 1991; 1993; Zhang et al., 1991; Zhu et al., 1991). Additionally, the amount of heparin required to induce a positive FGF-2 response (ng/ml) was well below the quantity reported to induce an FGF-2 dimer (μg/mL) (Ornitz et al., 1992, 1995). Therefore, the role of an FGF-2 oligomer in FGF-2 activity has been based purely on speculation. Our data clearly indicate that the *major* form of FGF-2 in the presence of equimolar amounts of a tetrasaccharide or a decasaccharide is a dimer or tetramer, respectively, and provide strong experimental evidence to support these previous speculations.

Interestingly, the three tetrasaccharide structures examined by Ornitz et al. (1995), one of which contains one of the most active trisaccharide sequences, had a 1000-fold decrease in FGF-2 binding relative to native heparin and did not facilitate binding to the soluble FGF receptor. It seems plausible that the mitogenetic activity exhibited by the di- and trisaccharides does not involve direct binding to FGF-2. But on the basis of these observations two distinct and opposed models were proposed by the authors where the role of heparin is either to stabilize self-associated FGF-2 oligomers by spanning adjacent primary heparin binding sites (Venkataraman et al., 1996) (beads-on-a-string model) or to stabilize self-associated FGF-2 dimers by binding to multiple heparin binding sites where the beads-on-a-string model is not the essential component of FGFR activation (Ornitz et al., 1995).

Our data indicate that the low levels of self-associated FGF-2 dimers present are not a significant component of the receptor active form of FGF-2 and heparin-induced improperly oriented FGF-2 dimers are not sufficient for biological activity. This is evident from the ability of the tetrasaccharide to dimerize FGF-2 without inducing a form of FGF-2 that binds to FGFR-1 and the fact that the self-associated dimer speculated to form in the presence of the di- and trisaccharides is not observed with the tetrasaccharide (Ornitz et al., 1995). Although the tetrasaccharide is too short to stabilize a preexisting FGF-2 dimer by binding to adjacent monomer heparin binding sites as proposed by Venkataraman et al. (1996), the tetrasaccharide is capable of inducing the sandwich motif dimer depicted in Figure 7. This sandwich dimer is completely unrelated to any self-associated FGF-2 dimer. Lack of evidence to indicate an association of the tetrasaccharide-induced sandwich dimer by FGF-2 self-association to form an "active" FGF-2 tetramer implies that spontaneous FGF-2 association may not play a significant role in the activation of FGF-2. This suggests that the functional role of heparin is to correctly orient and stabilize FGF-2 into the proper high-affinity dimer or tetramer configuration.

Our model also provides an interpretation to the observation that there are specific saccharide sequences that do not promote FGF-2−FGFR interaction, that is, failure to form the properly oriented FGF-2 dimer or tetramer complex (Aviezer et al., 1994). It is also in complete agreement with the isothermal titration calorimetry results for acidic fibroblast growth factor (FGF-1), where FGF-1 was shown to oligomerize in the presence of heparin and the extent of the oligomerization was dependent on the size of heparin. In addition, FGFR dimerization was only observed with heparin that caused oligomerization of FGF-1 (Spivak-Kroizman et al., 1994). The current study begins to define the nature of the FGF−2-HSPG−receptor complex, suggesting strategies for the design of chemical entities directed at specifically modulating the activity of the FGF-2 ligand−receptor system. This provides a mechanism to explain the functional interactions of heparin−HSPGs with FGF-2 which may be fundamental to this class of heparin binding growth factors. What is still undetermined for the FGF-2−HSPG−receptor complex is the relative orientation and specific interactions of the FGF-2−heparin dimer or tetramer complex with its receptor and the role of receptor−heparin interactions in FGF-2 activity.

ACKNOWLEDGMENT

We thank Dr. Dan Garrett and Frank Delaglio for the use of their programs for NMR data analysis and processing, Dr. Neil Farrow for the use of his programs for analysis of ^{15}N relaxation data, Dr. Robert J. Linhardt for providing the heparin-derived tetrasaccharide sample, and Dr. Carl Svahn for providing the heparin-derived decasaccharide.

SUPPORTING INFORMATION AVAILABLE

Figures showing the plot of χ^2 versus correlation time for free FGF-2 and the FGF-2−tetrasaccharide complex (1 page). Ordering information is given on any current masthead page.

REFERENCES

Ago, H., Kitagawa, Y., Fujishima, A., Matsuura, Y., & Katsube, Y. (1991) *J. Biochem. 110*, 360−363.
Aviezer, D., Levy, E., Safran, M., Svahn, C., Buddecke, E., Schmidt, A., David, G., Vlodavsky, I., & Yayon, A. (1994) *J. Biol. Chem. 269*, 114−121.
Baird, A., & Bohlen, P. (1990) in *Peptide Growth Factors and their Receptors* (Sporn, M., & Roberts, A., Eds.) *Handbook of Experimental Pharmacology*, vol. 95, No. 1, pp 369−418, Springer-Verlag, New York.
Basilico, C., & Moscatelli, D. (1992) *Adv. Cancer Res. 59*, 115−165.
Bodenhausen, G., & Ruben, D. J. (1980) *Chem. Phys. Lett. 69*, 185.
Clore, G. M., Driscoll, P. C., Wingfield, P. T., & Gronenborn, A. M. (1990a) *Biochemistry 29*, 7387−7401.
Clore, G. M., Szabo, A., Bax, A., Kay, L. E., Driscoll, P. C., & Gronenborn, A. M. (1990b) *J. Am. Chem. Soc 112*, 4989−4991.
Clubb, R. T., Omichinski, J. G., Sakaguchi, K., Appella, E., Gronenborn, A. M., & Clore, G. M. (1995) *Protein Sci. 4*, 855.
Delaglio, F., Grzesiek, S., Vuister, G. W., Zhu, G., Pfeifer, J., & Bax, A. (1995) *J. Biomol. NMR 6*, 277−293.
Eriksson, A. E., Cousens, L. S., Weaver, L. H., & Matthews, B. W. (1991) *Proc. Natl. Acad. Sci. U.S.A 88*, 3441−3445.
Eriksson, A. E., Cousens, L. S., & Matthews, B. W. (1993) *Protein Sci. 2*, 1274−1284.
Faham, S., Hileman, R. E., Fromm, J. R., Linhardt, R. J., & Rees, D. C. (1996) *Science 271*, 1116−1120.
Farrow, N. A., Muhandiram, R., Singer, A. U., Pascal, S. M., Kay, C. M., Gish, G., Shoelson, S. E., Pawson, T., Forman-Kay, J. D., & Kay, L. E. (1994) *Biochemistry 33*, 5984−6003.
Folkman, J., & Klagsbrun, M. (1987) *Science 235*, 442−447.
Garrett, D. S., Powers, R., Gronenborn, A. M., & Clore, G. M. (1991) *J. Magn. Reson. 95*, 214−220.
Gospodarowicz, D., & Cheng, J. (1986) *J. Cell. Physiol. 128*, 475−484.
Grzesiek, S., & Bax, A. (1993) *J. Am. Chem. Soc 115*, 12593−12594.
Ishihara, M., Tyrrell, D. J., Stauber, G. B., Brown, S., Cousens, L. S., & Stack, R. J. (1993) *J. Biol. Chem. 268*, 4675−4683.
Kamath, U., & Shriver, J. W. (1989) *J. Biol. Chem. 264*, 5586.
Kan, M., Wang, F., Xu, J., Crabb, J. W., Hou, J., & McKeehan, W. L. (1993) *Science 259*, 1918−1921.
Kay, L. E., Torchia, D. A., & Bax, A. (1989) *Biochemistry 28*, 8972−8979.
Kay, L. E., Nicholson, L. K., Delaglio, F., Bax, A., & Torchia, D. A. (1992) *J. Magn. Reson. 97*, 359−375.
Lappi, D. A., Maher, P. A., Martineau, D., & Baird, A. (1991) *J. Cell. Physiol. 147*, 17−26.
Li, L. Y., & Seddon, A. P. (1994) *Growth Factors 11*, 1−7.
Li, L. Y., Safran, M., Aviezer, D., Boehlen, P., Seddon, A. P., & Yayon, A. (1994) *Biochemistry 33*, 10999−11007.
Lipari, G., & Szabo, A. (1982) *J. Am. Chem. Soc. 104*, 4546−4559.
Maccarana, M., Casu, B., & Lindahl, U. (1993) *J. Biol. Chem. 268*, 23898−23905.
Mach, H., Volkin, D. B., Burke, C. J., & Middaugh, C. R. (1993) *Biochemistry 32*, 5480−5489.

Marion, D., Ikura, M., Tschudin, R., & Bax, A. (1989b) *J. Magn. Reson. 85*, 393−399.
Markley, J. L., Horsley, W. J., & Klein, M. P. (1971) *J. Chem. Phys. 55*, 3604.
Meiboom, S., & Gill, D. (1958) *Rev. Sci. Instrum 29*, 688.
Miyamoto, M., Naruo, K.-I., Seko, C., Matsumoto, S., Kondo, T., & Kurokawa, T. (1993) *Mol. Cell. Biol. 13*, 4251−4259.
Mohammadi, M., Schlessinger, J., & Hubbard, S. R. (1996) *Cell 86*, 577−587.
Moscatelli, D. (1987) *J. Cell. Physiol. 131*, 123−130.
Moy, F. J., Seddon, A. P., Campbell, E. B., Böhlen, P., & Powers, a. R. (1995) *J. Biomol. NMR 6*, 245−254.
Moy, F. J., Seddon, A. P., Böhlen, P., & Powers, R. (1996) *Biochemistry 35*, 13552−13561.
Nugent, M. A., & Edelman, E. R. (1992) *Biochemistry 31*, 8876−8883.
Ornitz, D. M., Yayon, A., Flanagan, J. G., Svahn, C. M., Levi, E., & Leder, P. (1992) *Mol. Cell. Biol. 12*, 240−247.
Ornitz, D. M., Herr, A. B., Nilsson, M., Westman, J., Svahn, C.-M., & Waksman, G. (1995) *Science 268*, 432−436.
Palmer, A. G. I., Rance, M., & Wright, P. E. (1991) *J. Am. Chem. Soc. 113*, 4371.
Pantoliano, M. W., Horlick, R. A., Springer, B. A., Van Dyk, D. E., Tobery, T., Wetmore, D. R., Lear, J. D., Nahapetian, A. T., Bradley, J. D., & Sisk, W. P. (1994) *Biochemistry 33*, 10229−10248.
Pervin, A., Gallo, C., Jandik, K. A., Han, X. J., & Linhardt, R. J. (1995) *Glycobiology 5*, 83−95.
Pineda-Lucena, A., Nunez de Castro, I., Lozano, R. M., Munoz-Willery, I., & Zazo, M. (1994) *Eur. J. Biochem. 222*, 425−431.
Piotto, M., Saudek, V., & Sklenar, V. (1992) *J. Biomol. NMR 2*, 661−665.
Powers, R., Clore, G. M., Stahl, S. J., Wingfield, P. T., & Gronenborn, A. (1992) *Biochemistry 31*, 9150−9157.
Press, W. M., Flannery, B. P., Teukolsky, S. A., & Vetterling, W. T. (1986) *Numerical Recipes*, Cambridge University Press, Cambridge.
Redfield, C., Boyd, J., Smith, L. J., Smith, R. A. G., & Dobson, C. M. (1992) *Biochemistry 31*, 10431.
Reiland, J., & Rapraeger, A. C. (1993) *J. Cell Sci. 105*, 1085−1093.
Roghani, M., & Moscatelli, D. (1992) *J. Biol. Chem. 267*, 22156−22162.
Saksela, O., Moscatelli, D., Sommer, A., & Rifkin, D. B. (1988) *J. Cell Biol. 107*, 743−751.
Sommer, A., & Rifkin, D. B. (1989) *J. Cell. Physiol. 138*, 215−220.
Spivak-Kroizman, T., Lemmon, M. A., Dikic, I., Ladbury, J. E., Pinchasi, D., Huang, J., Jaye, M., Crumley, G., Schlessinger, J., & Lax, I. (1994) *Cell 79*, 1015−1024.
Springer, B. A., Pantoliano, M. W., Barbera, F. A., Gunyuzlu, P. L., Thompson, L. D., Herblin, W. F., Rosenfeld, S. A., & Book, G. W. (1994) *J. Biol. Chem. 269*, 26879−26884.
Thompson, L. D., Pantoliano, M. W., & Springer, B. A. (1994) *Biochemistry 33*, 3831−3840.
Venkataraman, G., Sasisekharan, V., Herr, A. B., Ornitz, D. M., Waksman, G., Cooney, C. L., Langer, R., & Sasisekharan, R. (1996) *Proc. Natl. Acad. Sci. U.S.A. 93*, 845−850.
Westall, F. C., Rubin, R., & Gospodarowicz, D. (1983) *Life Sci. 33*, 2425−2429.
Xu, Z., Seddon, A., Kitchen, D., Bohlen, P., & Venkataraghavan, R. (1996) *Structure* (in preparation).
Yayon, A., Klagsbrun, M., Esko, J. D., Leder, P., & Ornitz, D. M. (1991) *Cell 64*, 841−848.
Yayon, A., Zimmer, Y., Shen, G. H., Avivi, A., Yarden, Y., & Givol, D. (1992) *EMBO J. 11*, 1885−1890.
Zhang, J., Cousens, L. S., Barr, P. J., & Sprang, S. R. (1991) *Proc. Natl. Acad. Sci. U.S.A 88*, 3446−3450.
Zhu, X., Komiya, H., Chirino, A., Faham, S., Fox, G. M., Arakawa, T., Hsu, B. T., & Rees, D. C. (1991) *Science 251*, 90−93.

BI9625455